Testing results and current status of FTS-2, an imaging Fourier transform spectrometer for SCUBA-2

Brad Gom[*a], David Naylor[a]
[a]Department of Physics, University of Lethbridge, Lethbridge, Alberta, Canada, T1K 3M4

ABSTRACT

The SCUBA-2 imaging Fourier Transform Spectrometer (FTS-2) is a dual-band Mach-Zehnder imaging spectrometer, built for use with the SCUBA-2 camera on the James Clerk Maxwell Telescope (JCMT). FTS-2 will provide resolving powers of R ~ 10 to 5000 across the 450 and 850 μm bands, with a FOV up to 5 arcmin^2. The instrument has been built and tested, with first light on the telescope planned for fall 2010. We present the alignment process, laboratory test results, and discuss the first science targets in the context of other similar space and ground-based instruments.

Keywords: Fourier, Spectrometer, SCUBA-2, Submillimetre, JCMT

1. INTRODUCTION

FTS-2 is an imaging Fourier transform spectrometer (FTS) which has been built for use with the SCUBA-2 camera[1] on the James Clerk Maxwell Telescope (JCMT). Laboratory integration and testing of FTS-2 has been completed, with installation and commissioning at the JCMT taking place in fall 2010 after the SCUBA-2 array upgrades. In this paper we discuss the laboratory testing results and planned first science targets. The design and modeled performance of the interferometer have been presented elsewhere[2,3].

A rendering of the FTS-2 system is shown in Figure 1, with the main subcomponents labeled. The FTS was designed as a modular system in order to simplify machining and shipping of such a large instrument (mass ~ 600 kg, volume ~ 2 m x 0.6 m x 1.3 m) The optics in the various modules (the folding mirrors in the interferometer arms, the beamsplitters, the pickoff mirrors, and the moving mirror assembly) are aligned and mounted separately to the optical breadboard, and then all components are aligned to each other using a coordinate measurement machine (CMM) inspection arm.

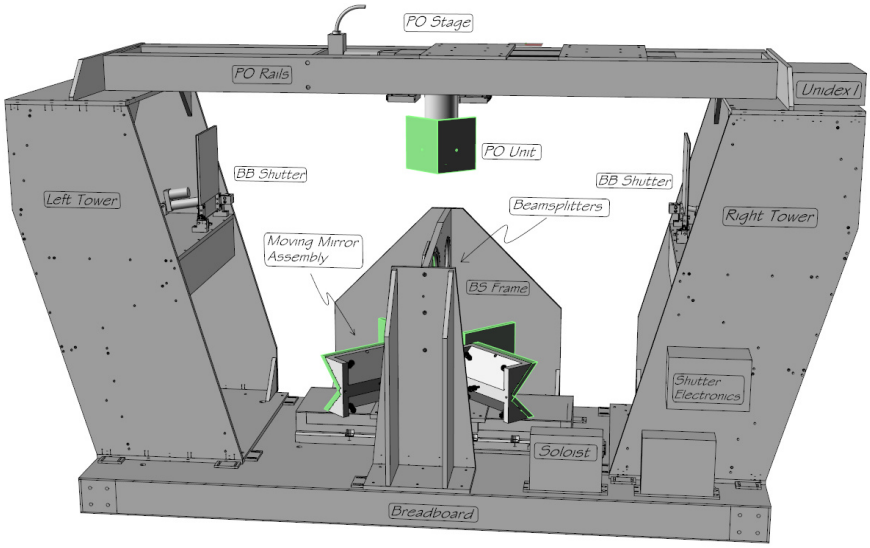

Figure 1. Rendering of the FTS-2 system, showing the main subcomponents. Light from the telescope is intercepted by the pickoff mirror unit, fed through the interferometer, and returned to the SCUBA-2 optical path (out of the page).

[*] brad.gom@uleth.ca; phone 1 403 329-2771; fax 1 403 329-2057; http://research.uleth.ca/scuba2/

FTS-2 was assembled, aligned and tested in the U of L labs, as shown in Figure 2. The shipping pallet doubles as a rigid mounting platform and ensures that the breadboard does not deflect during the alignment process. Strengthened plates on the four corners of the breadboard serve as hoist points for use with the JCMT overhead crane during installation on the telescope. Rails on the top of the instrument support a translation stage on which the pickoff mirror assembly is mounted (below, right). Piezo actuators are required for remote tip/tilt adjustment of each of the four pickoff mirrors, in order to align the instrument to the telescope after it is hoisted into position.

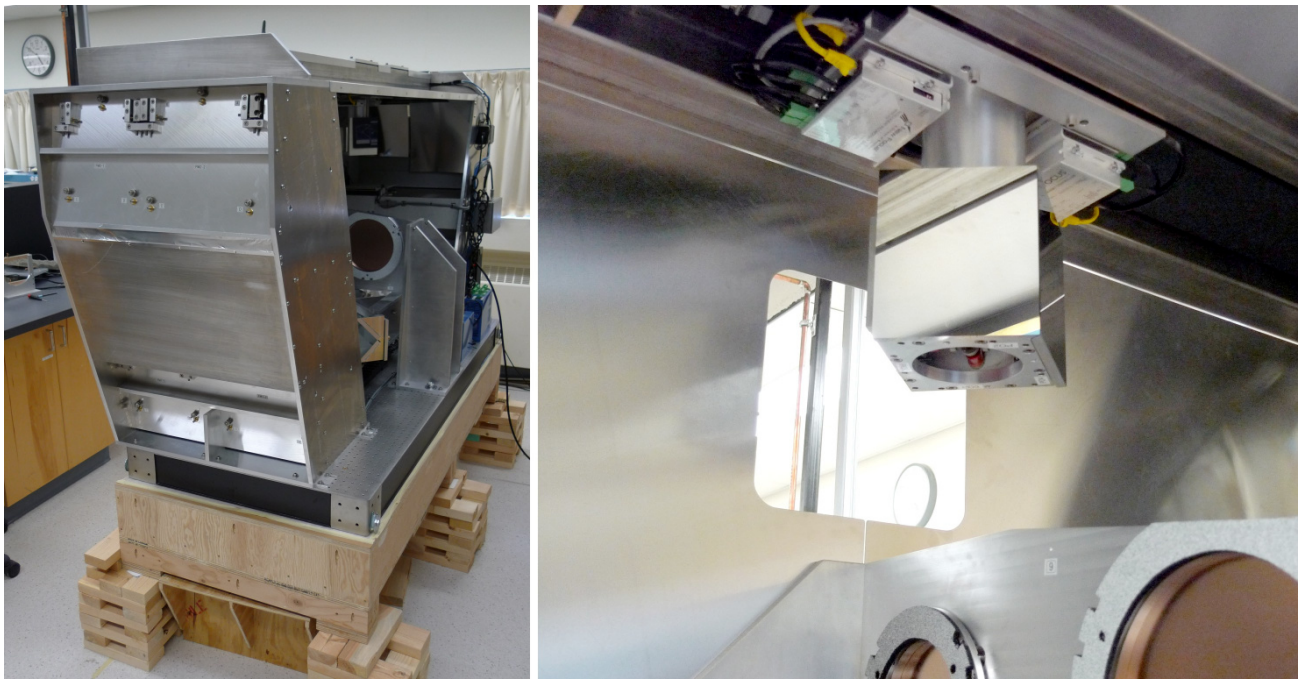

Figure 2. FTS-2 fully assembled on shipping platform (left). Adjusters for the fixed fold mirrors can be seen on the outside of the framework. A retractable pickoff mirror unit (right) allows SCUBA-2 to be used in photometric mode when the FTS is not in use.

Figure 3 shows the inside of the interferometer when the cover sheet metal is removed. Light from the telescope enters through the rectangular opening in the rear cover, reflects off the input pickoff mirrors towards the upper fixed aspherical fold mirrors (only the left arm of the interferometer is visible in the figure), through the input beamsplitter downwards towards the lower fold mirrors and moving corner-cube mirror assembly. The beam is sheared by the corner cube mirrors and directed through the output half of the interferometer and back to the output pickoff mirrors where it is returned to the SCUBA-2 optical train. Motorized ambient blackbody loads are mounted on each input of the interferometer, near the pupil locations in front of the fold mirrors. Both input ports of the Mach-Zehnder interferometer can be used simultaneously on the sky to provide instantaneous atmospheric cancellation, however, when the loads are inserted into the beam as shown below, the corresponding input can be blocked to provide calibration measurements or for operation of the FTS in single-input mode[4].

2. OPTICS

FTS-2 contains eighteen diamond-turned aluminum mirrors and two beamsplitters. Alignment of this many components in the interferometer requires a combination of optical and mechanical techniques. While the ten planar mirrors have optical quality surfaces, eight of the mirrors are aspherical and are not suitable for laser alignment due to the limitations of the freeform machining process. Alignment of the fixed mirrors is made possible by conical divots machined in the corners of the aspherical surfaces (shown in Figure 4). The form of the mirrors was measured relative to the divots using a small Microscribe CMM[5] which allows the mirror position and orientation to be determined relative to the mechanical structure using a larger CMM arm during the alignment process.

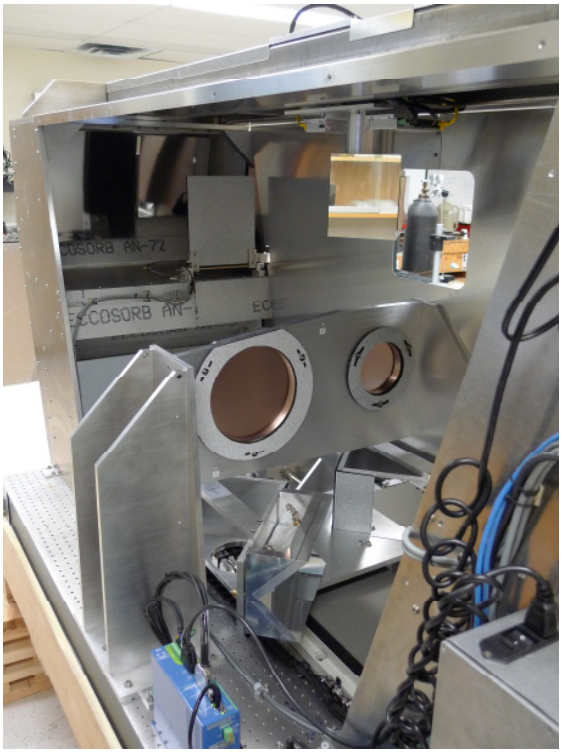

Figure 3. Inside of the FTS-2 system, showing the pickoff mirror unit and beamsplitters along the central plane of the interferometer, the moving corner-cube mirror assembly below the beamsplitters, and the fold mirrors in the left arm of the interferometer. The blackbody calibration load is shown inserted into the input beam.

Due to the large size of the optics (100 to 300 mm diameter) and tight space constraints for the instrument framework, mounts for the optics are integrated into the framework itself. Since the mirror coordinates are measured directly during the alignment process, compact mount designs could be used even though the adjusters over constrain the mirrors and do not act orthogonally to each other. Adjusters for one of the fixed mirrors are shown in Figure 4. Three springs hold the mirror against the adjusters. By removing the springs, the mirror can be removed and replaced without affecting the alignment. All actuators seat against stainless steel brackets or carbide inserts in the mirrors to avoid galling.

Figure 4. Freeform diamond-turned aspherical mirrors with locating divots in each corner (left). Each fixed mirror is aligned using 7 ball tipped adjusters in the support framework (right). Three adjusters for tip/tilt and displacement along the optical axis are labeled ‘T’, two adjusters for rotation about the optical axis and vertical displacement are labeled ‘V’, and two opposing adjusters for horizontal displacement are labeled ‘H’.

Alignment of the FTS optics is performed using a CMM arm which can reach each half of the interferometer in one setup. The CMM coordinate system is defined by locating divots on the main breadboard; all components are aligned to each other in this coordinate system. The alignment tolerances are +/-0.1° and +/-0.5 mm in displacement, which corresponds to a +/-0.1 mm tolerance in the measured absolute coordinates of the mirror locating divots. This tolerance within the 2 m x 1 m x 1 m volume of the FTS can just be met by current state of the art CMM arms. Since CMM arms use rotary encoders in their joints, the measurement tolerance generally decreases with the reach of the arm, and the accuracy achievable using a arm long enough to measure the full FTS in one setup is roughly the same as that which can be achieved using a shorter arm and 'leapfrogging' the arm coordinate system during the alignment process. The CMM arm used in the laboratory tests (Figure 5) had a 5 foot reach, which meant leapfrogging was required to reach both sides of the FTS, although the smaller size allowed the CMM to be mounted directly to the FTS breadboard.

Figure 5. CMM arm being used to measure the position of a locating divot in the corner of one of the fixed mirrors.

Alignment of the fixed mirrors is done iteratively by placing the probe tip in each mirror datum divot and turning the adjusters until the expected coordinates are achieved. This process is simplified if the CMM can be put in the local tilted coordinate system of each mirror, and the distance to the desired datum point is read out in that coordinate system. In this way, the required adjustment distances are in the same directions as the adjusters. Once all 8 fixed mirrors are adjusted, point-to-point measurements from mirrors on either side of the system are compared against the CAD model, ensuring that the global tolerances are met (+/- 0.1 mm XYZ).

Alignment of the corner cube moving mirror assembly is done before the assembly is installed in the FTS. Since the retroreflector is designed to shear the beam by 300 mm, there is a gap in the apices of the corner cubes. This gap complicates the autocollimation alignment process[6] when using an alignment telescope with diameter smaller than ~200 mm, so an alternative technique was used as shown in Figure 6. A reference corner cube with a closed apex and diameter large enough to span the gap in the FTS-2 corner cube was first aligned to a few arcsec (Figure 6a). The telescope was then offset to one side, and the sheared beam reflected from the corner cube was autocollimated with a plane mirror beside the telescope (Figure 6b). Finally, the FTS-2 corner cube could be aligned by placing it in front of the telescope as shown in (Figure 6c).

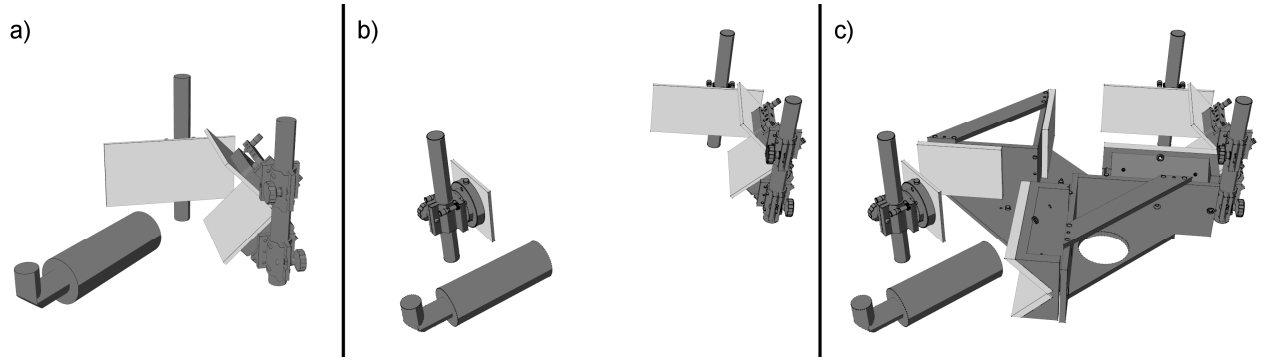

Figure 6. Alignment of the FTS-2 corner cube mirrors. a) A reference corner cube is aligned using a telescope with illuminated reticule. b) The telescope is offset to one side of the corner cube and a plane mirror is placed on the other side normal to the reflected, sheared beam. c) The FTS-2 corner cube assembly is placed in front of the telescope and aligned in order to restore the autocollimation produced in the previous step.

An optical alignment target is used to establish the position and angle of the FTS as a whole relative to the SCUBA-2 beam. A reflective circular target is held in a spring loaded retaining ring on a plate mounted to the FTS-2 beamsplitter framework. The position and angle of the target are set relative to the FTS coordinate system using the CMM during assembly, and then the target is sighted using the JAC Taylor-Hobson alignment scope from inside the telescope receiver cabin during installation. The FTS position and orientation are adjusted as required to bring the concentric rings of the target on-axis and perpendicular to the elevation bearing optical axis.

3. LABORATORY TEST RESULTS

Detailed results of the optical modeling and theoretical optical performance are presented elsewhere[7]; in this section we present a summary of the imaging and interferometric laboratory test results.

3.1 IR Imaging Performance

Although the aspherical mirror surface finish and the beamsplitter substrates preclude the use of optical imaging for alignment, thermal IR imaging can be used. A FLIR A320 camera operating at 7-14 μm was used to image one output for the FTS. With the pickoff mirror removed in order to have direct access to the input and output images, the camera was mounted on-axis with the central field of the output beam and aimed at the optical axis, as shown in the image below. The tip of a hot soldering iron placed at the input image plane could be easily seen in the output images.

Unfortunately, the ~25°×19° FOV and f/1.3 lens of the camera are not well matched to the SCUBA-2 system, so evaluation of spillover and vignetting was not possible. The array has 320x240 pixels, and each pixel corresponds to ~0.25 mm at the FTS output image plane. By comparison, the SCUBA-2 pixel size is ~2 mm at this image location. The FTS-2 output beam diameter is ~200 mm at the camera location, so the 35 mm diameter lens on the camera is not well matched to the FTS optics and only the central field is accurately represented in terms of vignetting and image geometry. Since the goal was to confirm the symmetry of the alignment in both halves of the FTS, however, only the central field was required. Image registration was confirmed using a heated Nichrome wire crosshair target placed on-axis at the input image plane. The true input and output image planes are curved, but a planar target can be used in the central region of the FOV for alignment purposes. The two halves of the interferometer were confirmed to be co-aligned to within ¼ of a SCUBA-2 pixel diameter.

3.2 Interferometric Performance

Imaging interferometric tests could not be performed using the IR camera due to the relatively low sensitivity and readout speed of the camera, as well as the poor performance of the beamsplitters at these wavelengths. Instead, a single-pixel pyroelectric detector was used to measure the interferogram of a 320 GHz line source[8] near the SCUBA-2 850 μm band. The source feedhorn was placed on-axis in the input image plane, and the detector was focused on the output image using a HDPE lens. Again, since proper telescope simulator optics were not available, only the on-axis performance could be evaluated.

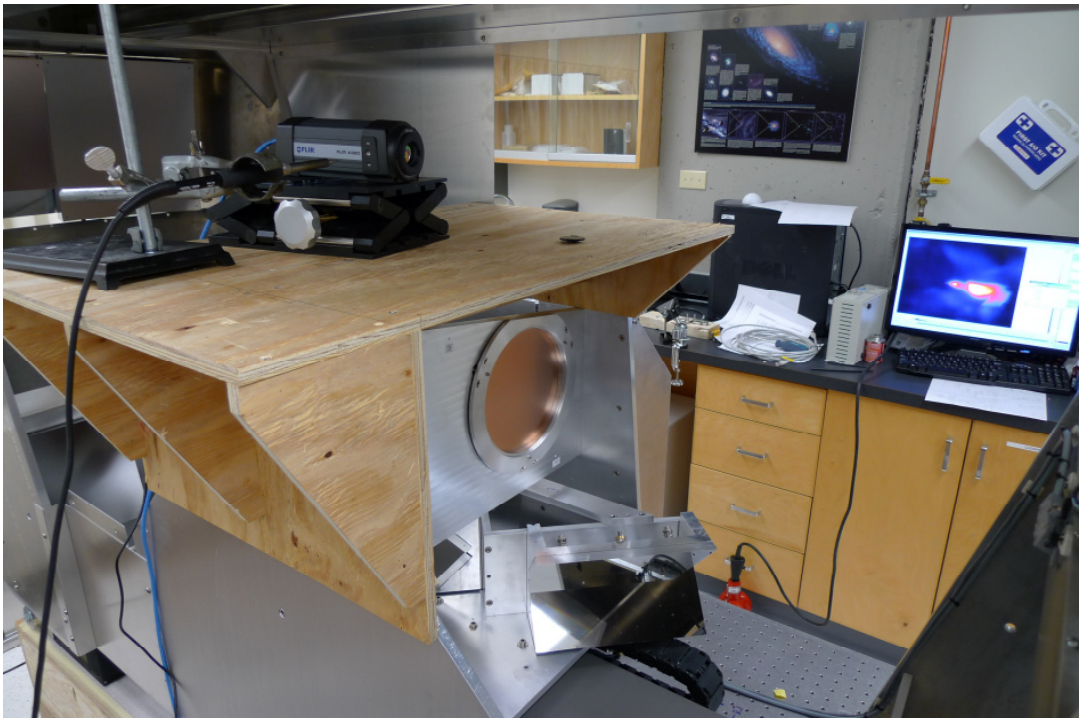

Figure 7. A thermal IR camera focused on the FTS output image plane with a hot soldering iron placed on the input image plane. The thermal image through both arms of the interferometer is shown on the screen in the background.

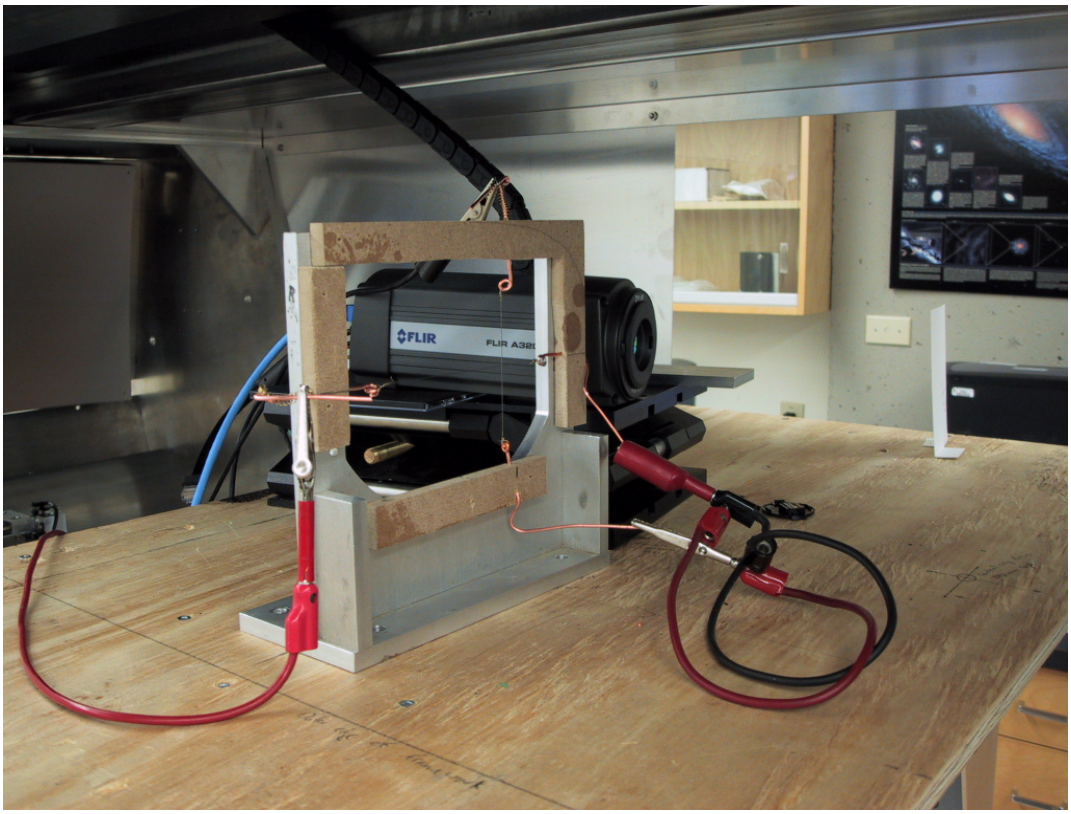

Figure 8. A pair of crossed Nichrome wires forms a heated crosshair target used with the IR camera to evaluate the image registration through the four paths through the interferometer.

The interferogram was sampled in the time domain since it was not possible to trigger the data acquisition system based on the translation stage position. When used with SCUBA-2, however, the FTS position values will be recorded for use to interpolate the time-domain interferogram onto a regularly spaced optical path difference grid. The raw power spectrum is shown in Figure 9 below. The measured line centre of 10.676 cm^{-1} is within 0.002 cm^{-1} of the true centre, well within the 0.006 cm^{-1} resolution of the FTS. Harmonics of the 320 GHz line can be seen in the spectrum which are most likely the result of position sampling jitter due to stage velocity variation during time domain sampling.

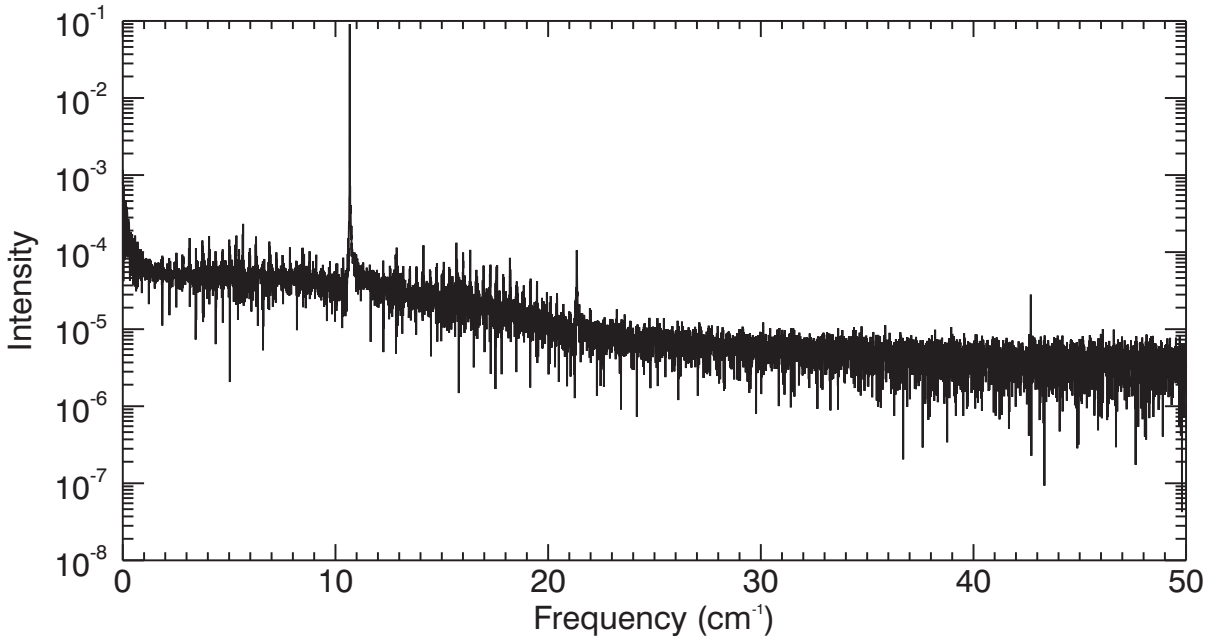

Figure 9. Measured spectrum of a 320 GHz line source placed on-axis with the FTS input. Echoes of the fundamental frequency can be seen as a result of translation stage velocity jitter.

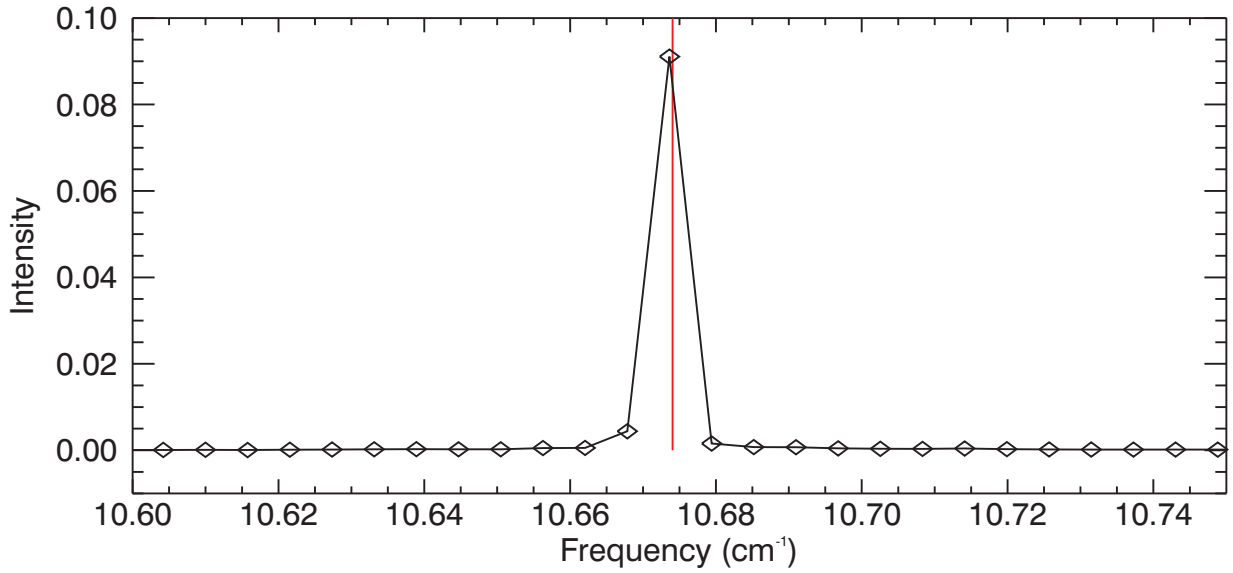

Figure 10. The line source frequency is plotted as a vertical line; the measured frequency of the unresolved line is well within the 0.006 cm^{-1} maximum resolution of the FTS.

By measuring the amplitude of the cosine interferogram signal over the full travel of the moving mirrors, the self apodization due to beam divergence and vignetting within the interferometer can be evaluated. The measured interferogram contrast ratio of ~0.9 at the maximum optical path difference is higher than the value of ~0.8 predicted by the optical model, as a result of the relatively large detector size and f/# of the source beam. The apodization function (Figure 11) is smooth over the travel of the moving mirrors, which confirms that there is no unusual vignetting within the system.

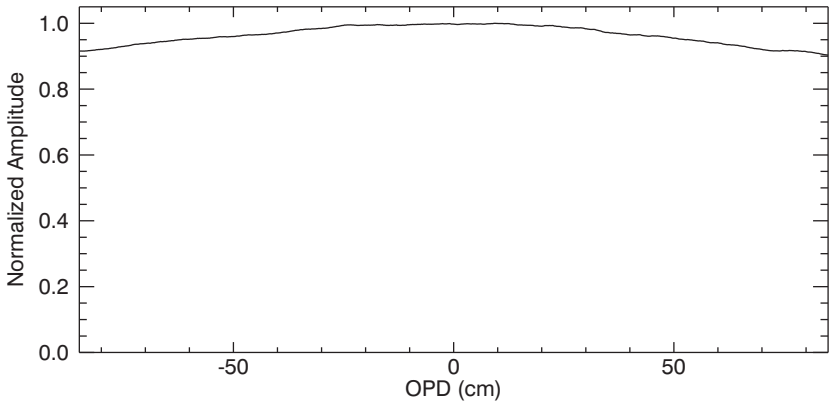

Figure 11. Interferogram amplitude (or contrast) as a function of optical path difference (OPD).

The instrumental lineshape produced by an ideal FTS is a sinc function. The measured lineshape of the phase-corrected spectrum matches an ideal sinc function very well, as shown in Figure 12.

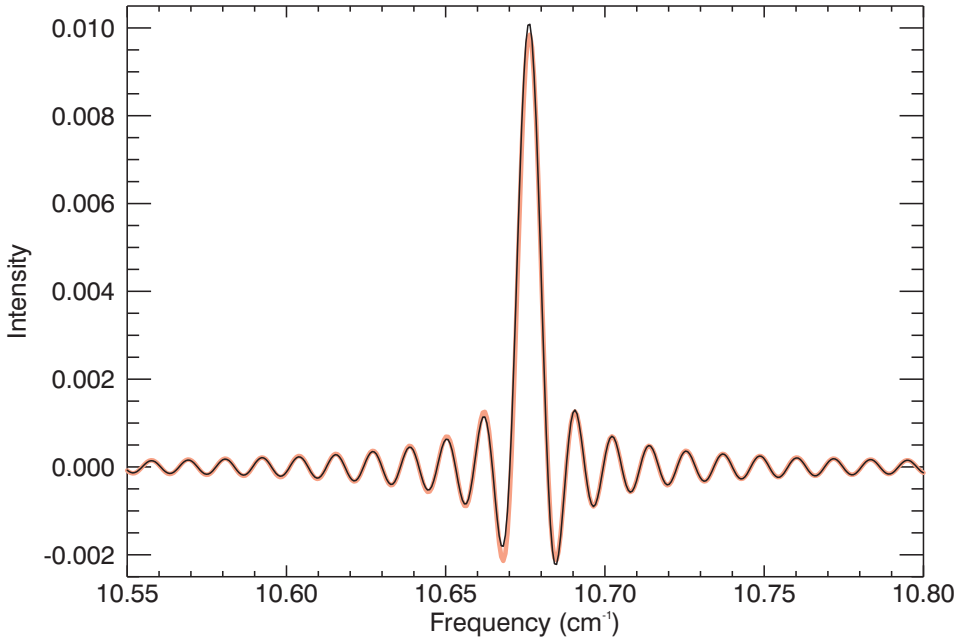

Figure 12. Measured ILS (thin line) plotted overtop of a sinc function corresponding to the theoretical resolution of the FTS (thick line). The interferogram has been sampled at uniform time intervals and full phase correction has not been applied.

Although the interferogram will be interpolated onto a uniform OPD grid when used with SCUBA-2, it is important that the time-sampled interferogram be sampled as regularly as possible. Since the power spectra shown above were recorded in the time domain, the size of the ghosts indicate that there is very little jitter in the moving mirror velocity. The velocity jitter can be characterized by plotting the measured fundamental line frequency over the travel of the moving mirrors, as shown in Figure 13. The frequency and therefore mirror speed and sampling uniformity is stable to ~0.2% RMS, well within tolerances of the interpolation algorithm.

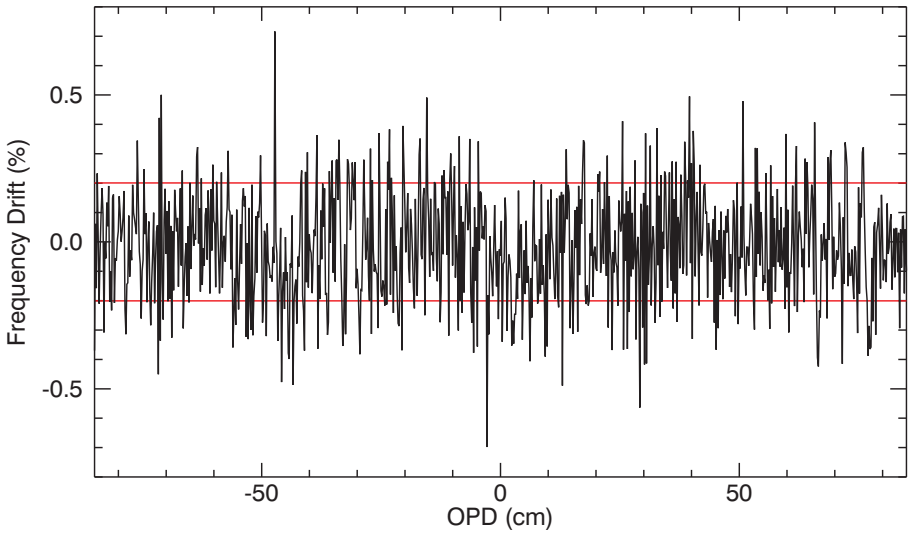

Figure 13. Measured drift of the fundamental line frequency during a high resolution scan. Horizontal lines indicate the RMS value.

4. SCIENCE TARGETS

The scientific aims of FTS-2 are to capitalize on the imaging power and sensitivity of the SCUBA-2 camera, and extend its capabilities to include simultaneous medium resolution imaging spectroscopy across the 450 and 850 μm atmospheric windows. The primary goal is to complement the large scale, photometric observations of SCUBA-2 and the small scale, high resolution, spectroscopic maps of HARP with large scale, intermediate resolution spectroscopic maps. Potential science targets for FTS-2 include:

- Planetary atmospheres, where the broad spectral coverage and intermediate resolution of FTS-2 is ideally suited to measuring the pressure broadened tropospheric absorption features
- The interstellar medium, where FTS-2 spectra can be analyzed to determine both the total continuum flux and its spectral index as well as the contribution from molecular line emission
- Extragalactic astronomy, where FTS-2 will be able to measure, simultaneously, the slope of the dust emissivity across both the 450 and 850 μm bands for the brightest ULIRGS.

With a single pointing, FTS-2 will be able to provide a spectrum at every point in the ~9 arcmin^2 field. Regardless of target, individual spectra can be analyzed to determine the total continuum flux and its spectral index, as well as the detection of strong emission lines. Such a data cube will provide a unique resource, unmatched by any other facility on any other telescope.

Since the atmosphere is the dominant source of emission at submillimetre wavelengths, FTS-2 was designed to place its two input ports on the sky to remove the common mode atmospheric signal. However, since FTS-2 measures the difference between the radiation entering both ports, this makes observations of extended sources challenging. Observations with FTS-2 must therefore be carefully planned, using prior knowledge of the source region, to determine the optimum observing time and strategy.

To illustrate this problem, Figure 14 shows an 850 μm map of part of the Orion molecular cloud taken with SCUBA[9]. Superimposed on this map are two circles representing the two input ports of FTS-2, one of which remains centred on the source region under study, while the second port moves in an arc around the pointing centre over the course of a long integration due to sky rotation. In addition to cancelling out the common mode atmospheric signal, FTS-2 will take the spectral difference between astronomical sources in the two ports. For point-like sources this does not present a serious limitation, but it has to be considered when using FTS-2 to observe extended sources. In practice it is expected that any FTS-2 observation will be planned based on a prior photometric measurement with SCUBA-2 to assess the impact of unwanted source radiation in the second port.

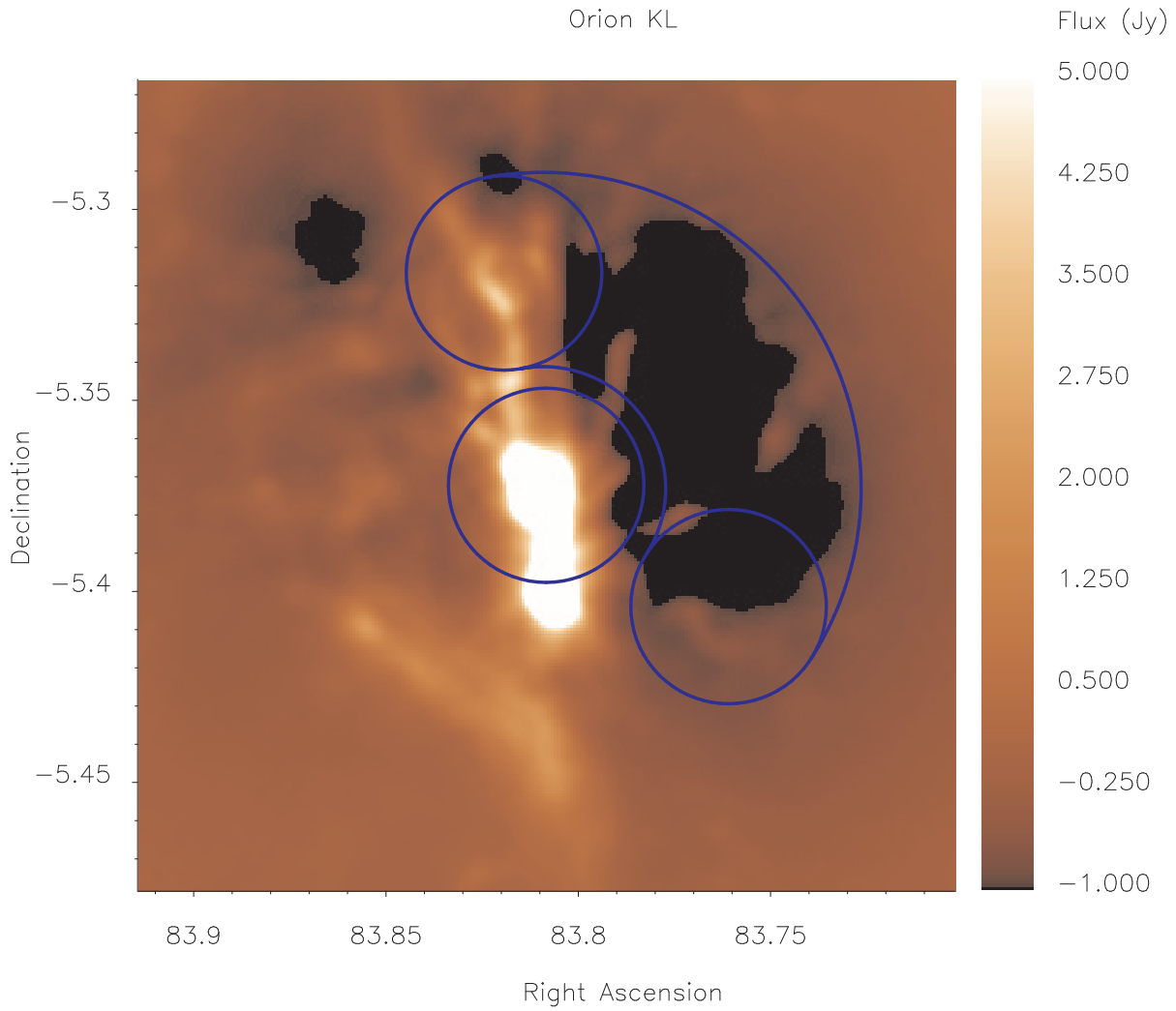

Figure 14. Example of the impact of port rotation on measurements of an extended source. The target is located at the centre of the fixed circle, while the second port of FTS-2 rotates in an arc around the pointing centre. The upper extreme of the arc contains significant source emission which would produce erroneous results in the difference signal.

In order to simulate realistic FTS-2 spectra, we have used spectra of the Orion KL region (the source shown in Figure 14) obtained with the JCMT facility detector RxB3. This spectrum, shown in the upper plot of Figure 15 has been convolved with the measured instrumental lineshape (Figure 12) and subsampled to yield a realistic estimate of the spectrum that will be observed with FTS-2. The complex spectrum with its negative lobes, well known attributes of the sinc function, may appear noisy to layperson. However, with a detailed knowledge of the ILS, it is possible to retrieve quantitative spectral information.

A sophisticated spectral line fitting routine that our group has developed for the Herschel SPIRE instrument has been used to analyze the simulated spectrum of Orion. The 10 strongest spectral lines shown in the lower plot of Figure 15 were fitted. The results of the fit and the component decomposition are shown in Figure 16. The retrieved spectral parameters are listed in Table 1. It can be seen that in all cases the line centres are recovered to better than ~10% of a spectral resolution element. The uncertainties in the retrieved integrated line fluxes, not unexpectedly, depend on the line strength. Yet even in such a complex spectrum the results show that FTS-2 is capable of providing quantitative spectral information

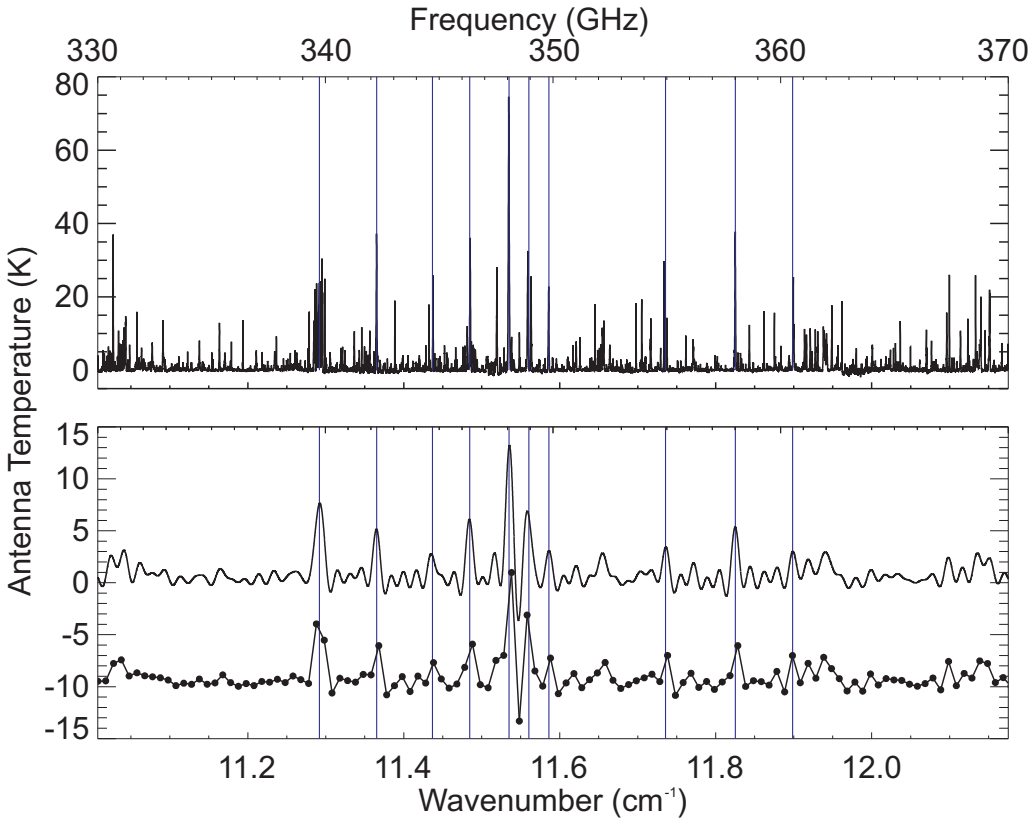

Figure 15. Heterodyne spectrum of the Orion Kl region obtained using RxB3 (upper plot). Simulated FTS-2 spectrum resulting from the convolution of the ILS (see Figure 12) with the heterodyne spectrum.

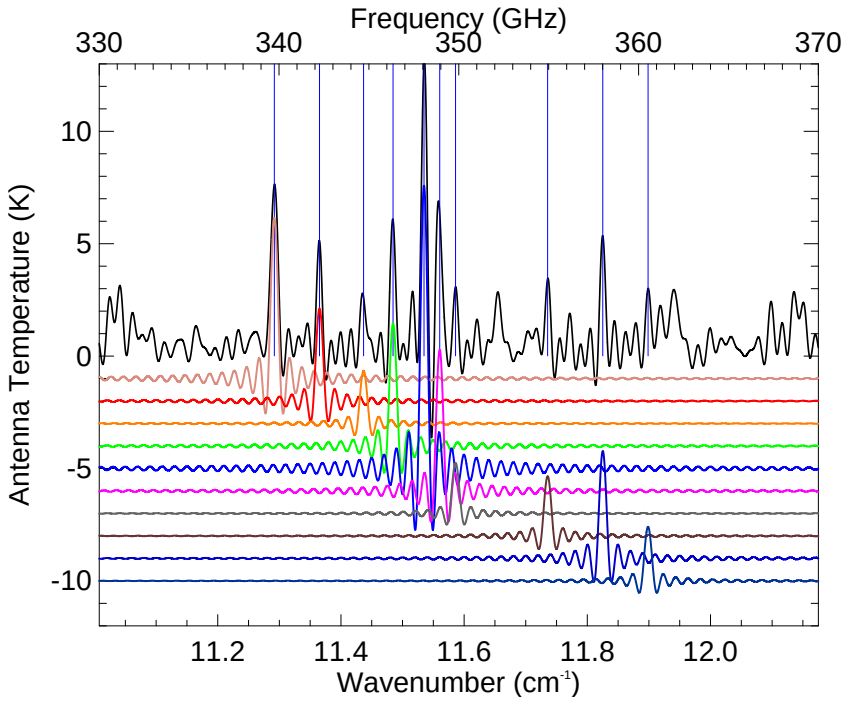

Figure 16. Results of the application of line fitting routine to identify the 10 strongest lines in the simulated spectrum of Figure 15.

Table 1. Comparison of the line centre and integrated flux from the Heterodyne and FTS spectra of Figure 15. For the line centres, the error is given relative to a spectral resolution element of 0.01 cm^{-1}. The error in the integrated line area is calculated relative to the heterodyne values.

	Line Centre (cm^{-1})			Integrated Line Area (mK cm^{-1})		
Line	Heterodyne	FTS	% Error	Heterodyne	FTS	% Error
1	11.29190	11.29186	0.43	70.6014	72.6704	2.93
2	11.36507	11.36524	1.69	40.2619	34.1113	15.28
3	11.43739	11.43677	6.24	16.6701	19.4588	16.73
4	11.48509	11.48465	4.45	38.7520	45.2157	16.68
5	11.53455	11.53491	3.61	105.8352	104.2260	1.52
6	11.56100	11.56037	6.34	62.9778	52.0161	17.41
7	11.58583	11.58612	2.88	23.9017	18.6604	21.93
8	11.73500	11.73558	5.78	27.2739	22.0401	19.19
9	11.82500	11.82512	1.23	39.9138	39.5709	0.86
10	11.89970	11.89861	10.95	22.3851	19.9303	10.97

While the final sensitivity of FTS-2 will only be known following commissioning after the SCUBA-2 science-grade array upgrades, current models predict that a spectral sensitivity of ~50 mJy per resolution element of 3 GHz (0.1 cm^{-1}), 5σ per hour, in the 850 μm band, will be achieved. The spectral sensitivity in the 450 μm band is typically much worse, being heavily dependent on the poor transmission of this atmospheric window; models predict an equivalent spectral sensitivity of ~ 250 mJy per resolution element.

5. CONCLUSION

Laboratory integration and testing of FTS-2, the imaging spectrometer for SCUBA-2, is complete and the instrument has successfully passed its laboratory acceptance review. The spectrometer is being shipped to the JCMT where it will be installed and commissioned in fall 2010.

6. ACKNOWLEDGEMENTS

On behalf of the Canadian SCUBA-2 consortium, the authors acknowledge the support of a CFI international access award for Canadian participation in the SCUBA-2 project. David Naylor acknowledges support from NSERC. The authors also acknowledge the work of Regan Dahl in testing the control software, Scott Jones for help with sensitivity modeling, Peter Ade and Carole Tucker for providing the beamsplitters, and the review panels for their constructive input and encouragement

REFERENCES

[1] Holland, W.S., Duncan, W.D., Kelley, B.D., Irwin, K.D., Walton, A.J., Ade, P.A.R., and Robson, E.I., "SCUBA-2: A large format submillimetre camera on the James Clerk Maxwell Telescope", Proc. SPIE 4855, 1-18 (2003).
[2] Leclerc, M.R., Gom, B.G., Naylor, D.A., "Optical design of the SCUBA-2 IFTS", Proc. SPIE 7014, (2008).
[3] Gom, B.G., Naylor, D.A, Zhang, B., "Integration and testing of FTS-2: an imaging Fourier transform spectrometer for SCUBA-2", Proc. SPIE 7020, (2008).
[4] Gom, B.G., Naylor, D.A. "An update on the imaging Fourier transform spectrometer for SCUBA-2", Proc. SPIE 5498, 695-704 (2004).
[5] http://www.emicroscribe.com/products/microscribe-mx.htm
[6] Naylor, D.A., Schultz, A.A., "A simple technique for accurately measuring the dihedral angle of a roof-top mirror", Optics and Photonics News 11, (2000).
[7] Leclerc, M.R., Gom, B.G., Naylor, D.A., "Optical Design of the SCUBA-2 IFTS", Proc. SPIE 7014, 701471 (2008).
[8] http://www.virginiadiodes.com
[9] Johnstone, D. Bally, J., "JCMT/SCUBA Submillimeter Wavelength Imaging of the Integral-shaped Filament in Orion", Ap. J., 510, L49-53, (1999).